Root-specific activation of plasma membrane H^+-ATPase 1 enhances plant growth and shoot accumulation of nutrient elements under nutrient-poor conditions in *Arabidopsis thaliana*

Kota Monden[a], Takehiro Kamiya[b], Daisuke Sugiura[c], Takamasa Suzuki[d], Tsuyoshi Nakagawa[a] and Takushi Hachiya[a†]

[a]Department of Molecular and Functional Genomics, Interdisciplinary Center for Science Research, Shimane University, Matsue 690-8504, Japan

[b]Graduate School of Agricultural and Life Sciences, The University of Tokyo, Tokyo 113-8657, Japan

[c]Graduate School of Bioagricultural Sciences, Nagoya University, Nagoya 464-8601, Japan

[d]College of Bioscience and Biotechnology, Chubu University, Kasugai 487-8501, Japan

[†]To whom correspondence should be addressed.

E-mail: takushi.hachiya@life.shimane-u.ac.jp

Tel.: +81-852-32-6288

Fax: +81-852-32-6109

Abbreviations: GO, Gene Ontology; NUE, Nutrient uptake efficiency; PCA, Principal component analysis; PM, plasma membrane; RPM, Reads per million mapped reads; RT, Reverse transcription; SA, Salicylic acid; SAR, Systemic acquired resistance; WT, Wild-type

Abstract

Plasma membrane (PM) H^+-ATPase contributes to nutrient uptake and stomatal opening by creating proton gradient across the membrane. Previous studies report that a dominant mutation in the *OPEN STOMATA2* locus (*OST2-2D*) constitutively activates *Arabidopsis* PM H^+-ATPase 1 (AHA1), which enlarges proton motive force for root nutrient uptake. However, the stomatal opening is also constitutively enhanced in the *ost2-2D*, causing drought hypersensitivity. To develop plants with improved nutrient acquisition and normal stomatal movement, we generated grafted plants (scion/rootstock : Col-0 (WT)/*ost2-2D*), and compared their growth and nutrient element content with those of control plants (WT/WT) under two nutrient regimes. WT/*ost2-2D* shoots had larger weights, rosette diameter, leaf blade area, and content of C, N, K, Ca, S, P, Mg, Na, Mn, B, Co, and Mo under nutrient-poor conditions compared with WT/WT shoots. The root weights and primary root length were greater in WT/*ost2-2D* plants than in WT/WT plants under both nutrient conditions. These results suggest that root-specific activation of PM H^+-ATPase enhances root nutrient uptake, which accelerates the plant growth under nutrient-poor condition. Our study presents a novel approach to improving nutrient uptake efficiency in crops and vegetable for the implementation of low-input sustainable agriculture.

Keywords: *Arabidopsis thaliana*; micrografting; nutrient uptake efficiency; OPEN STOMATA 2; plasma membrane H^+-ATPase

46 **1. Introduction**

47 A growing population requires agriculture to increase crop production on a global scale. Nutrient
48 availability is an important determinant of crop productivity; thus, fertilizers are often applied in large
49 amounts to improve crop production. Intensive fertilizer use, however, puts a heavy burden on the
50 environment, e.g., through groundwater pollution, eutrophication, and greenhouse gas emissions [1].
51 N, P, and K, macronutrients typically in high demand in plants, account for a major portion of applied
52 fertilizers. The artificial synthesis of N fertilizers requires massive fossil fuel consumption; i.e.,
53 ammonia synthesis via the Harber–Bosch process consumes 1%–2% of the global energy budget
54 currently [2]. Additionally, the P contained in fertilizers is derived from nonrenewable rock phosphate
55 that will be depleted in the future [3]. Thus, developing plants with high nutrient uptake efficiency
56 (NUE) is crucial to achieving sustainable agriculture.

57 It is widely accepted that plasma membrane (PM) H^+-ATPase provides proton motive force
58 for root nutrient uptake mediated by specific transporters and channels [4]. Constitutive
59 overexpression of *Oryza sativa* PM H^+-ATPase 1 (*OSA1*) under the control of the *CaMV-35S* promoter
60 was shown to enhance root uptake of ammonium, plant growth, and productivity in both the field and
61 laboratory [5]. Conversely, similar overexpression of PM H^+-ATPase genes failed to confer any
62 positive effects on *Arabidopsis* and tobacco plants [6, 7]. Importantly, post-translational activation of
63 PM H^+-ATPase often has major effects on *Arabidopsis* physiological responses, including stomatal
64 opening and hypocotyl elongation [8, 9]. Therefore, with the aim of improving the NUE of
65 *Arabidopsis*, we focused on the *Arabidopsis OPEN STOMATA 2* (*OST2*)-dominant mutant (*ost2-2D*),
66 which expresses a constitutively active allele of the *Arabidopsis* PM H^+-ATPase 1 (*AHA1*) [9]. This
67 mutant exhibits lower apoplastic pH and longer-sized root epidermal cells, corresponding to
68 enhancements in proton motive force and acid growth in the roots, respectively [10]. However, PM
69 hyperpolarization in the guard cells of *ost2-2D* causes drought hypersensitivity due to the prevention
70 of stomatal closure, even with the addition of abscisic acid [9, 11, 12]. Thus, the root-specific
71 activation of OST2/AHA1 could be an ideal design for improving NUE. To achieve this design, we
72 grafted Col-0 (wild-type; WT) scions onto rootstock originating from WT or *ost2-2D* and analyzed

73 the vegetative growth, nutrient element content, and transcriptomes of the grafted plants grown under
74 nutrient-rich or nutrient-poor conditions. We show that *ost2-2D*-derived rootstock enhances the
75 growth of shoots and roots as well as the shoot accumulation of several nutrient elements under
76 nutrient-poor conditions.

77

78 **2. Materials and methods**

79 *2.1. Plant materials and growth conditions*

80 Seeds of Col-0 (WT) and *ost2-2D* [9] were surface sterilized and sown in a solid medium containing
81 50 mL of half-strength Murashige and Skoog (1/2-MS) salts including vitamins (Code M0222;
82 Duchefa Biochemie, Haarlem, The Netherlands) supplemented with 0.05% (w/v) MES-KOH (pH 5.7),
83 1% (w/v) sucrose, and 0.5% (w/v) gellan gum (Fujifilm Wako, Osaka, Japan). The seeds were placed
84 in the dark at 4°C for 3 days to break dormancy. Seedlings were grown vertically under a PPFD of
85 25 μmol m^{-2} s^{-1} (16/8-h light/dark cycle) at 22°C. Micrografting was performed aseptically using 5-
86 day-old seedlings [13], which were cut perpendicularly in the hypocotyl with an injection needle tip
87 (Code NN-2613S; TERUMO, Tokyo, Japan). The obtained scion was connected with the partner
88 rootstock in a silicon microtube (Code 1-8194-04; AS ONE, Osaka, Japan). The grafted plants were
89 incubated for 5 days under a PPDF of 50 μmol m^{-2} s^{-1} (constant light) at 27°C and further cultivated
90 for 1 day under a PPFD of 25 μmol m^{-2} s^{-1} (16/8-h light/dark cycle) at 22°C except that the grafted
91 plants used for the measurement of root length were not subjected to cultivation for 1 day under a
92 PPFD of 25 μmol m^{-2} s^{-1} (16/8-h light/dark cycle) at 22°C. Successfully grafted plants without
93 adventitious root formation were selected for similar size; transferred to vermiculite pots, soil pots, or
94 solid media; and grown for use in the following experiments. For vermiculite cultivation, the grafted
95 plants were grown under a PPFD of 100–120 μmol m^{-2} s^{-1} (16/8-h light/dark cycle) at 22°C–23°C.
96 Before the cultivation, ~150 mL of vermiculite was soaked with 80 mL of 1/2-MS or 1/50-MS salts
97 without vitamins (Code M0221; Duchefa Biochemie) supplemented with 0.05% (w/v) MES-KOH (pH
98 5.7). Four days after the onset of cultivation, 30 mL of the same compositions of 1/2-MS or 1/50-MS

salts was supplied to the vermiculite. The plants were then cultivated for an additional 3 days; after which, they were sampled for experiments. For soil cultivation, the grafted plants were grown for 7 days under a PPFD of 100–120 μmol m^{-2} s^{-1} (16/8-h light/dark cycle) at 22°C–23°C in the pots containing ~150 mL of nutrient-rich soil (Supermix A; Sakata Seed, Kyoto, Japan). For an *in vitro* culture on solid media, the plants were grown for 3 days (vertically) or 7 days (horizontally) under a PPFD of 100–120 μmol m^{-2} s^{-1} (16/8-h light/dark cycle) at 22°C–23°C in 30 mL (horizontally) or 50 mL (vertically) of 1/2-MS or 1/50-MS salts without vitamins (Duchefa Biochemie) supplemented with 0.05% (w/v) MES-KOH (pH 5.7), 1% (w/v) sucrose, and 0.8% (w/v) purified agar (Code 01162-15; Nacalai Tesque, Kyoto, Japan). To allow nondestructive sampling of the roots, the surfaces of solid media were covered with cellophane sheets [14]. All other details are described in the figure legends.

2.2. Growth analysis of plants under vermiculite and soil cultivation

Shoots were weighed on a precision balance (HR-202i; A&D, Tokyo, Japan) and scanned at a resolution of 600 dpi (GT-X980; EPSON, Tokyo, Japan) to measure rosette diameter. Leaf blades were harvested from the shoots and scanned at a resolution of 600 dpi to measure the area of the leaf blades. The shoots were then oven-dried at 80°C for 2 days and recovered in a desiccator with silica gel. Shoot dry weights were measured using the precision balance, and the rosette diameter and leaf blade area were measured using ImageJ version 1.52p.

2.3. Growth analysis of plants under in vitro culture on solid media

The shoots and roots of horizontally grown plants were weighed using the precision balance, after which they were oven-dried at 80°C for 2 days and recovered in a desiccator with silica gel. The dry weights of the shoots and roots were measured using the precision balance. The roots of vertically grown plants were scanned at a resolution of 600 dpi to measure the length of primary and lateral roots (>0.3 mm). Root length was measured using ImageJ version 1.52p.

126 *2.4. Determination of nutrient elements*

127 Harvested shoots were oven-dried at 80°C for 2 days, and the dried samples were ground using a
128 spoon and recovered in a desiccator with silica gel. For determination of C and N, the dried powder
129 was weighed and encapsulated in a tin boat, and C and N concentrations were measured using a CN
130 analyzer (Vario EL III; Elementar Analysensysteme GmbH, Hanau, Germany). For determination of
131 K, P, S, Ca, Fe, Mg, Mn, Na, B, Co, Cu, Mo, and Zn, the dried samples were weighed and digested
132 using 2 mL of concentrated HNO_3 followed by the addition of 1 mL of H_2O_2 at 120°C until it
133 evaporated. The digested samples were dissolved in 0.08 M HNO_3 and the element concentrations
134 were measured using inductively coupled plasma–mass spectrometry (Agilent 7800 ICP-MS; Agilent
135 Technologies, Santa Clara, CA, USA) using 2 ppb indium as an internal standard.

136

137 *2.5. Extraction of total RNA*

138 Roots were harvested, immediately frozen using liquid N_2, and stored at −80°C until use. Frozen
139 samples were ground with a Multi-Beads Shocker (Yasui Kikai, Osaka, Japan) using zirconia beads
140 (diameter: 5 mm). Total RNA was extracted using an RNeasy Plant Mini Kit (Qiagen, Tokyo, Japan)
141 according to the manufacturer's instructions. For RNA-Seq library preparation, RNA was purified
142 using on-column DNase digestion (Qiagen).

143

144 *2.6. RT-qPCR*

145 Reverse transcription (RT) was performed using ReverTra Ace qPCR RT Master Mix with gDNA
146 Remover (Toyobo, Osaka Japan) according to the manufacturer's instructions. The synthesized cDNA
147 was diluted 10-fold with distilled water and used in quantitative PCR (qPCR). RT-qPCR was
148 performed on a QuantStudio 1 (Thermo Fisher Scientific) with KOD SYBR qPCR Mix (Toyobo)
149 according to the manufacturer's instructions. Transcript levels were quantified using a relative standard
150 curve with *ACTIN3* as the internal standard [19]. Primer sequences are shown in Supplementary Table
151 1.

152

153 *2.7. RNA-Seq analysis*

154 RNA quality was evaluated using a Qubit RNA IQ Assay Kit with a Qubit 4 Fluorometer (Thermo
155 Fisher Scientific, Tokyo, Japan). The RNA samples for which RNA IQs were 9.1–10.0 were used for
156 the following preparation. cDNA libraries were constructed using a NEBNext Ultra II RNA Library
157 Prep with Sample Purification Beads (Code E7775; New England Biolabs, Tokyo, Japan), a NEBNext
158 Poly(A) mRNA Magnetic Isolation Module (Code E7490; New England Biolabs), and a NEBNext
159 Multiplex Oligos for Illumina (Index Primers Set 3) (Code E7710; New England Biolabs) according
160 to the manufacturer's instructions. These cDNA libraries were sequenced using NextSeq 500 (Illumina,
161 Tokyo, Japan), and the produced bcl files were converted to fastq files using bcl2fastq (Illumina). The
162 resulting sequence data have been stored in the ArrayExpress (https://www.ebi.ac.uk/arrayexpress/)
163 under the accession number (E-MTAB-11843). The reads were analyzed according to the method
164 described by Notaguchi et al. [15] and mapped to the *Arabidopsis* reference (TAIR10) using Bowtie
165 [16] with the following options: "--all --best --strata." The number of reads mapped to each reference
166 was counted, and the obtained read counts were processed and analyzed using the iDEP ver. 095
167 integrated web application [17] with the default settings. Pathway enrichment analyses were
168 performed using the Metascape web application with the default settings [18]. Information about read
169 counts is provided in Supplementary Table 2.

170

171 *2.8. Statistical analysis*

172 Unpaired two-tailed Welch's *t*-tests were conducted using R v.2.15.3.

173

174 **3. Results**

175 *3.1. Confirmation of root-specific missense mutation of OST2/AHA1*

176 To manipulate the activity of OST2/AHA1 in a root-specific manner, we grafted WT scions onto
177 rootstock originating from WT or *ost2-2D* (Supplementary Fig. 1A). To confirm the missense
178 mutation (G867S) of *OST2/AHA1* reported previously [9], we extracted RNA from the shoots and

179 roots of grafted plants (scion/rootstock: WT/WT and WT/*ost2-2D*). RT-PCR was performed using
180 primers specific to *OST2*/*AHA1*; after which, the PCR products were sequenced directly. The missense
181 mutation was detected only in the cDNA derived from the WT/*ost2-2D* roots (Supplementary Fig. 1B).
182
183 *3.2. Root-specific activation of OST2/AHA1 enhances shoot growth under nutrient-poor conditions*
184 Grafted plants were transferred to vermiculite pots to analyze the effects of root-specific activation of
185 OST2/AHA1 on shoot growth. Following cultivation for 7 days under nutrient-rich (1/2-MS salts) or
186 nutrient-poor conditions (1/50-MS salts), shoot growth was analyzed. WT/*ost2-2D* plants exhibited
187 increased shoot growth relative to that of WT/WT plants under 1/50-MS but not 1/2-MS conditions
188 (Fig. 1A). Under 1/50-MS conditions, shoot fresh and dry weights were significantly increased by
189 28% and 31%, respectively, in WT/*ost2-2D* plants than in WT/WT plants (Fig. 1A). Additionally,
190 rosette diameter and leaf blade area were significantly increased by 13% and 29%, respectively, in
191 WT/*ost2-2D* plants than in WT/WT plants under 1/50-MS conditions (Fig. 1A). Under 1/2-MS
192 conditions, however, only the shoot dry weight was significantly increased by 11% in WT/*ost2-2D*
193 plants (Fig. 1A). When the grafted plants were grown in pots containing nutrient-rich soil or in solid
194 media containing 1/2-MS or 1/50-MS, the shoot fresh and dry weights, rosette diameter, and leaf blade
195 area in WT/*ost2-2D* plants were slightly, albeit not always significantly, increased compared with
196 those in WT/WT plants (Supplementary Fig. 2A, B). Relative water content of shoots did not
197 substantially decrease in WT/*ost2-2D* plants compared with those in WT/WT plants regardless of
198 nutritional availability and cultivation style (Supplementary Fig. 3A–C). Thus, root-specific activation
199 of OST2/AHA1 does not cause shoot desiccation due to excessive stomatal opening.
200
201 *3.3. Root-specific activation of OST2/AHA1 enhances root growth irrespective of nutrient availability*
202 Barbez et al. [10] reported that the epidermal cell length of the primary roots of *ost2-2D* seedlings is
203 significantly larger than that of WT plants, suggesting that root growth is altered because of root-
204 specific activation of OST2/AHA1. To confirm this, the root growth of grafted plants grown vertically
205 on solid media containing 1/2-MS or 1/50-MS salts was analyzed. The appearance of the roots in

206 WT/WT plants differed according to nutrient condition, and their fresh and dry weights and lateral
207 root length were generally increased under 1/50-MS conditions than under 1/2-MS conditions (Fig.
208 1B and Supplementary Fig. 4A). In WT/*ost2-2D* plants relative to in WT/WT plants, root fresh weight
209 and root dry weight were significantly increased by 30% and 41% under 1/2-MS conditions,
210 respectively, and by 28% and 23% under 1/50-MS conditions, respectively (Fig. 1B). The primary
211 root length was significantly increased in WT/*ost2-2D* plants by 22% and 32% under 1/2-MS and
212 1/50-MS conditions, respectively; however, no significant difference was observed in the lateral root
213 length of the grafted plants (Fig. 1B). In grafted plants grown horizontally on solid media, root fresh
214 and dry weights were increased in WT/*ost2-2D* plants than in WT/WT plants irrespective of nutrient
215 availability (Supplementary Fig. 4B).
216
217 *3.4. Root-specific activation of OST2/AHA1 increases the shoot content of nutrient elements*
218 Zhang et al. [5] reported that constitutive overexpression of *OSA1* significantly increases the content
219 of C, N, K, P, and Ca in the leaves of rice grown in nutrient-rich hydroponic solution. Thus, we
220 determined the content of C and the 14 nutrient elements contained in MS salts in the shoots of grafted
221 plants grown in vermiculite. The content of C, N, K, Ca, S, P, Mg, Na, Mn, B, Co, and Mo was
222 significantly increased in WT/*ost2-2D* shoots than in WT/WT shoots under 1/50-MS conditions (Fig.
223 2). In particular, the content of macronutrients N, K, Ca, S, and P was consistently increased by 54%,
224 37%, 24%, 31%, and 44%, respectively, in WT/*ost2-2D* shoots than in WT/WT shoots (Fig. 2). Under
225 1/2-MS conditions, however, only Na content was significantly increased in the WT/*ost2-2D* shoots
226 than in the WT/WT shoots, although several elements showed increasing trends in the WT/*ost2-2D*
227 shoots (Fig. 2). The shoot concentrations of nutrient elements were generally comparable between the
228 grafted plants regardless of nutrient availability (Supplementary Fig. 5).
229
230 *3.5. Root-specific activation of OST2/AHA1 alters root expression of genes related to biotic responses*
231 To explore the effects of root-specific activation of *OST2/AHA1* on the root transcriptome, we
232 performed RNA-Seq analysis on the roots of grafted plants grown horizontally on solid media

233 containing 1/2-MS or 1/50-MS salts. Hierarchical clustering and principal component analysis (PCA)
234 classified the RNA-Seq data into four groups according to genotype and nutrient condition
235 (Supplementary Fig. 6A, B). The k-means clustering analysis revealed two gene clusters for which the
236 expression was induced (cluster 2) or repressed (cluster 3) in WT/*ost2-2D* roots than in WT/WT roots
237 (Fig. 3A, B and Supplementary Table 2). Each cluster was characterized using pathway enrichment
238 analysis; cluster 2 was enriched in Gene Ontology (GO) terms associated with systemic acquired
239 resistance (SAR) and responses to fungal infection, whereas cluster 3 was enriched in the GO term
240 "lipid X metabolic process" (Fig. 3C). The expression of multiple genes encoding UDP-3-*O*-acyl N-
241 acetylglycosamine deacetylase family proteins LPXC1–5, which contribute to the biosynthesis of lipid
242 X, a precursor of lipid A-like molecules [20], was consistently repressed in WT/*ost2-2D* roots
243 (Supplementary Fig. 7A, B), although the physiological roles played by endogenous lipid A-like
244 molecules are unknown.

245

246 **4. Discussion**

247 The present study demonstrates that root-specific activation of OST2/AHA1 enhances shoot growth
248 and increases the shoot content of all the macronutrient elements and six micronutrient elements in *A.*
249 *thaliana* cultivated in nutrient-poor vermiculite (Figs. 1A and 2). The root-specific activation of
250 OST2/AHA1 also increased root weight and primary root length in plants grown in solid media (Fig.
251 1B and Supplementary Fig. 4), corresponding to root cell expansion due to apoplastic acidification,
252 i.e., acid growth [10]. Given that the availability of nutrient elements limits plant vegetative growth
253 under nutrient-poor conditions, the improvement of proton motive force and root growth could
254 facilitate nutrient uptake and shoot growth. In the present study, the concentrations of N, K, P, Mg, B,
255 and Mo in WT/WT shoots were decreased by 19%–53% when nutrient availability was reduced
256 (Supplementary Fig. 5), suggesting that the supply of these elements could limit shoot growth under
257 nutrient-poor conditions. Because the shoot content of N, K, P, Mg, B, and Mo was consistently
258 increased in WT/*ost2-2D* plants than in WT/WT plants (Fig. 2), root-specific activation of

259 OST2/AHA1 may enhance shoot growth by increasing root uptake of these elements. Interestingly,
260 root expression of the high-affinity nitrate uptake transporter *NRT2.1* and iron uptake transporter *IRT1*
261 was higher in WT/*ost2-2D* plants than in WT/WT plants under nutrient-poor conditions
262 (Supplementary Fig. 8A, B). IRT1 has broad specificity for divalent heavy metals other than Fe
263 including Mn, Zn, Co, and Cd under Fe-deficient conditions [21]. Therefore, up-regulation of *NRT2.1*
264 and *IRT1* might have contributed to increases in the shoot content of N, Mn, and Co under nutrient-
265 poor conditions (Fig. 2).

266 Our transcriptome analysis suggested that root-specific activation of OST2/AHA1 up-
267 regulates genes related to SAR and fungal infection responses in the roots (Fig. 3C). This corresponds
268 to an observation made previously that salicylic acid (SA) levels and expression of SA-responsive
269 marker genes are elevated in the leaves of *ost2-1D* mutants [9], because endogenous SA acts as a
270 signal that mediates local and systemic defense responses to pathogen infection [22]. Interestingly,
271 lowering the pH in external media *per se* is known to induce expression of genes responsive to
272 pathogens, pathogen elicitors, and SA in *A. thaliana* roots [23]. Therefore, root-specific activation of
273 OST2/AHA1 may up-regulate expression of these genes through apoplastic acidification [10].

274 In conclusion, we succeeded in increasing plant vegetative growth under nutrient-poor conditions via
275 root-specific activation of PM H^+-ATPase using a grafting strategy. Genome editing technologies are
276 applicable for substituting specific DNA sequences for a gene of interest in various plant species;
277 therefore, it may be possible to design and produce rootstocks with activated PM H^+-ATPase. Overall,
278 our study presents a novel approach to improving NUE in crops and vegetables; thus, it could
279 contribute to the implementation of low-input sustainable agriculture.

280

281 **Acknowledgments**

282 Seeds of *ost2-2D* were kindly provided by Dr. Jeffrey Leung (CNRS, France). We thank Maki Saiki
283 for ICP-MS analysis. The authors would like to thank Enago (www.enago.jp) for the English language
284 review.

Funding

This study was supported by a KAKENHI Grant from Japan Society for the Promotion of Science [Grant-in-Aid for Scientific Research (C) No. JP20K05771 to TH] and the Ichimura Foundation for New Technology (to TH).

Conflict of interest

The authors declare that this study was conducted in the absence of any commercial relationships that could lead to any potential conflicts of interest.

References

[1] S. Savci, An Agricultural Pollutant: Chemical Fertilizer, Int. J. Environ. Sci. Dev. 3 (2012) 77-80. https://doi.org/10.7763/IJESD.2012.V3.191.

[2] V. Kyriakou, I. Garagounis, A. Vourros, et al., An Electrochemical Haber-Bosch Process, Joule 277 (2020) 142-158. https://doi.org/10.1016/j.joule.2019.10.006.

[3] J. Cooper, R. Lombardi, D. Boardman, et al., The future distribution and production of global phosphate rock reserves, Resour. Conserv. Recycl. 57 (2011) 78–86. https://doi.org/10.1016/j.resconrec.2011.09.009.

[4] M. G. Palmgren, Plant plasma membrane H^+-ATPases: powerhouses for nutrient uptake, Annu. Rev.Plant Biol. 52 (2001) 817–845. https://doi.org/10.1146/annurev.arplant.52.1.817.

[5] M. Zhang, Y. Wang, X. Chen, et al., Plasma membrane H^+-ATPase overexpression increases rice yield via simultaneous enhancement of nutrient uptake and photosynthesis, Nat. Commun. 12 (2021) 735. https://doi.org/10.1038/s41467-021-20964-4.

[6] M. Hashimoto-Sugimoto, T. Higaki, T. Yaeno, et al., A Munc13-like protein in *Arabidopsis* mediates H^+-ATPase translocation that is essential for stomatal responses, Nat. Commun. 4 (2013) 2215. https://doi.org/10.1038/ncomms3215.

[7] F. Gévaudant, G. Duby, E. von Stedingk, et al., Expression of a Constitutively Activated Plasma Membrane H^+-ATPase Alters Plant Development and Increases Salt Tolerance, Plant

313 Physiol. 144 (2007) 1763–1776. https://doi.org/10.1104/pp.107.103762.
314 [8] J. Falhof, J. T. Pedersen, A. T. Fuglsang, et al., Plasma Membrane H^+-ATPase Regulation in
315 the Center of Plant Physiology, Mol. Plant 9 (2016) 323–337.
316 https://doi.org/10.1016/j.molp.2015.11.002.
317 [9] S. Merlot, N. Leonhardt, F. Fenzi, et al., Constitutive activation of a plasma membrane H^+-
318 ATPase prevents abscisic acid-mediated stomatal closure, EMBO J. 26 (2007) 3216–3226.
319 https://doi.org/10.1038/sj.emboj.7601750.
320 [10] E. Barbez, K. Dünser, A. Gaidora, et al., Auxin steers root cell expansion via apoplastic pH
321 regulation in *Arabidopsis thaliana*, Proc. Natl. Acad. Sci. USA. 114 (2017) E4884–E4893.
322 https://doi.org/10.1073/pnas.1613499114.
323 [11] S. D'Alessandro, Y. Mizokami, B. Légeret, et al., The Apocarotenoid β-Cyclocitric Acid
324 Elicits Drought Tolerance in Plants, iScience 19 (2019) 461–473.
325 https://doi.org/10.1016/j.isci.2019.08.003.
326 [12] J. H. Wong, M. Klejchová, S. A. Snipes, et al., SAUR proteins and PP2C.D phosphatases
327 regulate H^+-ATPases and K^+ channels to control stomatal movements, Plant Physiol. 185
328 (2021) 256–273. https://doi.org/10.1093/plphys/kiaa023.
329 [13] K. Monden, M. Kojima, Y. Takebayashi, et al., Root-specific Reduction of Cytokinin
330 Perception Enhances Shoot Growth in *Arabidopsis thaliana*, Plant Cell Physiol. (2022) 256–
331 273. https://doi.org/10.1093/pcp/pcac013.
332 [14] T. Hachiya, T. Oya, K. Monden, et al., A cellophane-supported *Arabidopsis* culture for
333 seamless transfer between different media is useful for studying various nitrogen responses,
334 Soil Sci. Plant Nutr. 67 (2021) 277–282. https://doi.org/10.1080/00380768.2021.1908094.
335 [15] M. Notaguchi, T. Higashiyama, T. Suzuki, Identification of mRNAs that move over long
336 distances using an RNA-Seq analysis of *Arabidopsis/Nicotiana* benthamiana heterografts,
337 Plant Cell Physiol. 56 (2014) 311–321. https://doi.org/10.1093/pcp/pcu210.
338 [16] B. Langmead, C. Trapnell, M. Pop, et al., Ultrafast and memory-efficient alignment of short
339 DNA sequences to the human genome, Genome Biol. 10 (2009) R25.
340 https://doi.org/10.1186/gb-2009-10-3-r25.
341 [17] S. X. Ge, E. W. Son, R. Yao, iDEP: an integrated web application for differential expression
342 and pathway analysis of RNA-Seq data, BMC Bioinform. 19 (2018) 534.
343 https://doi.org/10.1186/s12859-018-2486-6.
344 [18] Y. Zhou, B. Zhou, L. Pache, et al., Metascape provides a biologist-oriented resource for the
345 analysis of systems-level datasets, Nat. Commun. 10 (2019) 1523.

346 https://doi.org/10.1038/s41467-019-09234-6.
347 [19] T. Hachiya, J. Inaba, M. Wakazaki, et al., Excessive ammonium assimilation by plastidic
348 glutamine synthetase causes ammonium toxicity in *Arabidopsis thaliana*, Nat. Commun. 12
349 (2021) 4944. https://doi.org/10.1038/s41467-021-25238-7.
350 [20] C. Li, Z. Guan, D. Liu, et al., Pathway for lipid A biosynthesis in *Arabidopsis thaliana*
351 resembling that of *Escherichia coli*, Proc. Natl. Acad. Sci. USA. 108 (2011) 11387–11392.
352 https://doi.org/10.1073/pnas.1108840108.
353 [21] A. Jogawat, B. Yadav, Chhaya, et al., Metal transporters in organelles and their roles in heavy
354 metaltransportation and sequestration mechanisms in plants, Physiol. Plant 173 (2021) 259–
355 275. https://doi.org/10.1111/ppl.13370.
356 [22] D. F. Klessig, H. W. Choi, D. A. Dempsey, et al., Systemic Acquired Resistance and Salicylic
357 Acid:Past, Present, and Future, Mol. Plant Microbe Interact. 31 (2018) 871–888.
358 https://doi.org/10.1094/MPMI-03-18-0067-CR.
359 [23] I. D. A. Lager, O. Andréasson, T. L. Dunbar, et al., Changes in external pH rapidly alter plant
360 gene expression and modulate auxin and elicitor responses, Plant Cell Environ. 33
361 (2010)1513–1528. https://doi.org/10.1111/j.1365-3040.2010.02161.x.

362

363 **Figure legends**

364 **Fig. 1. Effects of root-specific activation of OST2/AHA1 on the growth of shoots and roots.** (A)
365 Shoot appearance, shoot fresh and dry weights, rosette diameter, and leaf blade area of the grafted
366 plants. Grafted plants were transferred to vermiculite pots and grown for 7 days with a supply of 1/2-
367 MS or 1/50-MS salts. All data pooled from six independent grafting experiments are presented as
368 means ± SD (n = 43–44). (B) Root fresh and dry weights and primary and lateral root lengths of
369 grafted plants. Grafted plants were transferred to 1/2-MS or 1/50-MS media and grown vertically for
370 3 days. All data pooled from four independent grafting experiments are presented as means ± SD
371 (n = 30). WT/WT (W/W) and WT/*ost2-2D* (W/*o*) denote plants corresponding to the WT scion grafted
372 on the WT rootstock and the WT scion grafted on the *ost2-2D* rootstock, respectively. *$P < 0.05$;
373 ***$P < 0.001$; NS, not significant at $P > 0.05$ (unpaired two-tailed Welch's *t*-test). Scale bar: 0.5 cm.
374

375 **Fig. 2. Effects of root-specific activation of OST2/AHA1 on the shoot content of nutrient**
376 **elements.** The shoot content of 15 nutrient elements in the grafted plants, which were transferred to
377 vermiculite pots and grown for 7 days with a supply of 1/2-MS or 1/50-MS salts. Shoot samples
378 harvested from three (for C and N determination) and five (for determination of the other elements)
379 independent grafting experiments were subjected to element analysis. Shoots from 4 to 11 plants in
380 each experiment were pooled as one biological replicate. Data are presented as means ± SD (n = 3 or
381 5). WT/WT (W/W) and WT/*ost2-2D* (W/*o*) denote the plants corresponding to the WT scion grafted
382 on the WT rootstock and the WT scion grafted on the *ost2-2D* rootstock, respectively. *$P < 0.05$;
383 **$P < 0.01$; NS† $P < 0.1$; NS, not significant at $P > 0.05$ (unpaired two-tailed Welch's *t*-test).
384
385 **Fig. 3. Effects of root-specific activation of OST2/AHA1 on the root transcriptome.** (A) Heat map
386 from k-means clustering, (B) violin plots of normalized transcript levels in clusters 2 and 3, and (C)
387 pathway enrichment analyses of the genes in clusters 2 and 3. Grafted plants were transferred to 1/2-
388 MS or 1/50-MS media and grown horizontally for 7 days. Root samples harvested from two
389 independent grafting experiments were subjected to RNA-Seq analysis. Roots from four plants in each
390 experiment were pooled as one biological replicate. Genes for which the standard deviation was
391 ranked in the top 2000 were used for k-means clustering with four clusters, which included 769, 288,
392 219, and 724 genes (clusters 1–4), respectively. Purple and green represent higher and lower
393 expressions, respectively. Information about genes included in each cluster is provided in
394 Supplementary Table 3. Pathway enrichment analyses were performed using the obtained clusters 2
395 and 3, and significantly enriched terms are shown. WT/WT (W/W) and WT/*ost2-2D* (W/*o*) denote
396 plants corresponding to the WT scion grafted on the WT rootstock and the WT scion grafted on the
397 *ost2-2D* rootstock, respectively.

Figure 1

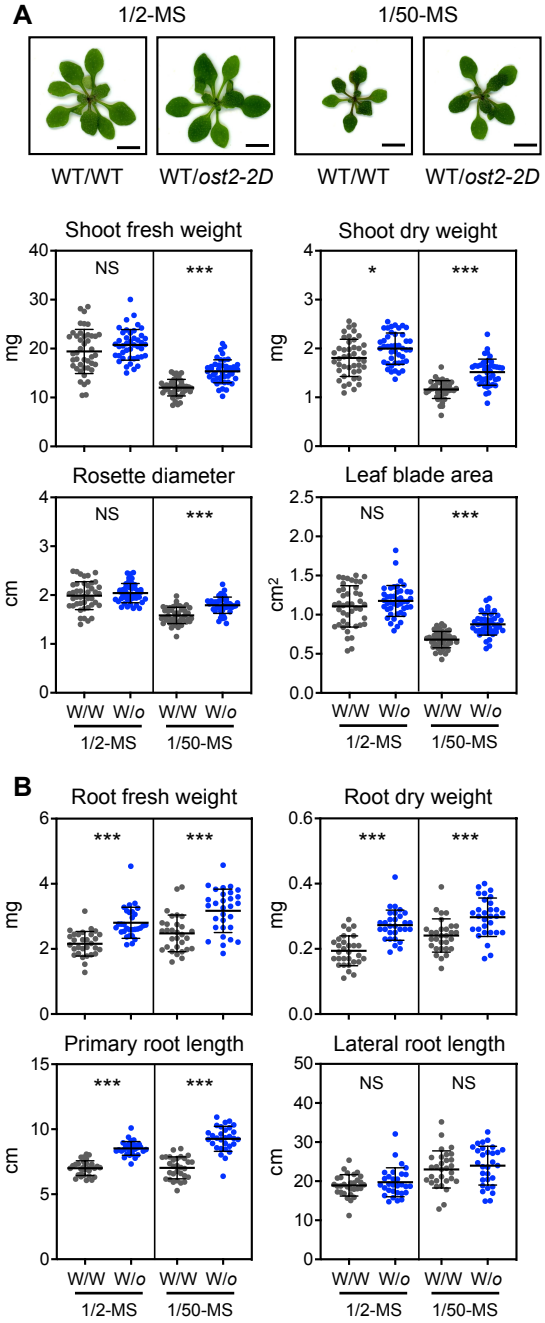
A
1/2-MS
1/50-MS
WT/WT
WT/ost2-2D
WT/WT
WT/ost2-2D
Shoot fresh weight
Shoot dry weight
Rosette diameter
Leaf blade area
mg
cm
cm2
NS
***
*
W/W
W/o
1/2-MS
1/50-MS
B
Root fresh weight
Root dry weight
Primary root length
Lateral root length

Figure 2

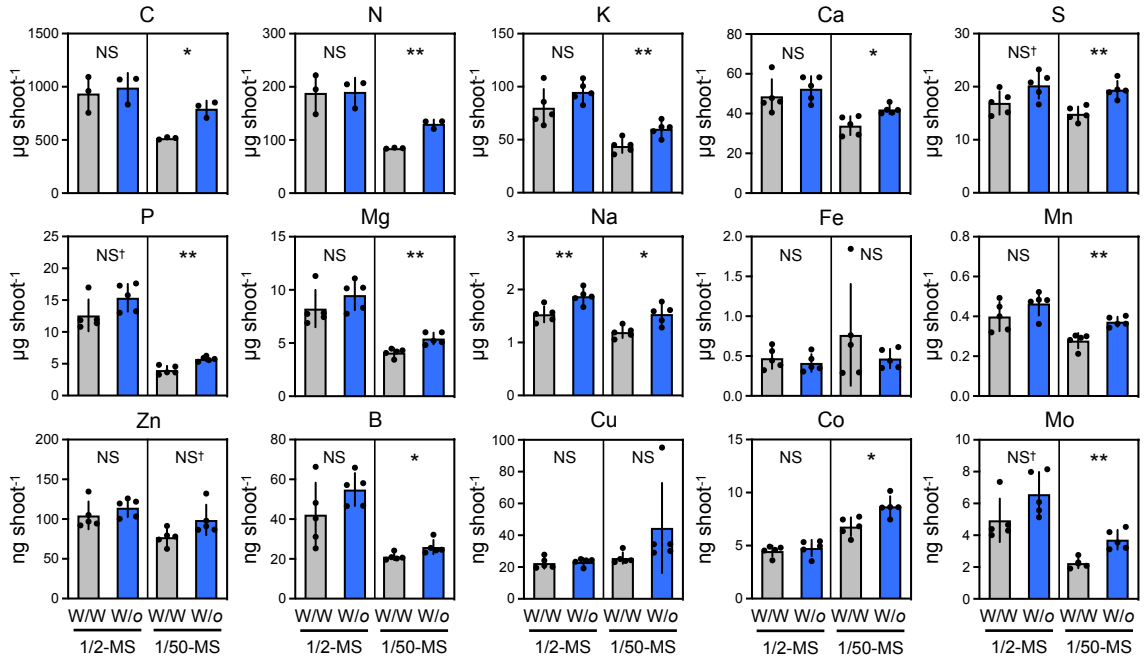
C
N
K
Ca
S
P
Mg
Na
Fe
Mn
Zn
B
Cu
Co
Mo
μg shoot-1
ng shoot-1
NS
NS†
*
**
W/W
W/o
1/2-MS
1/50-MS

Figure 3

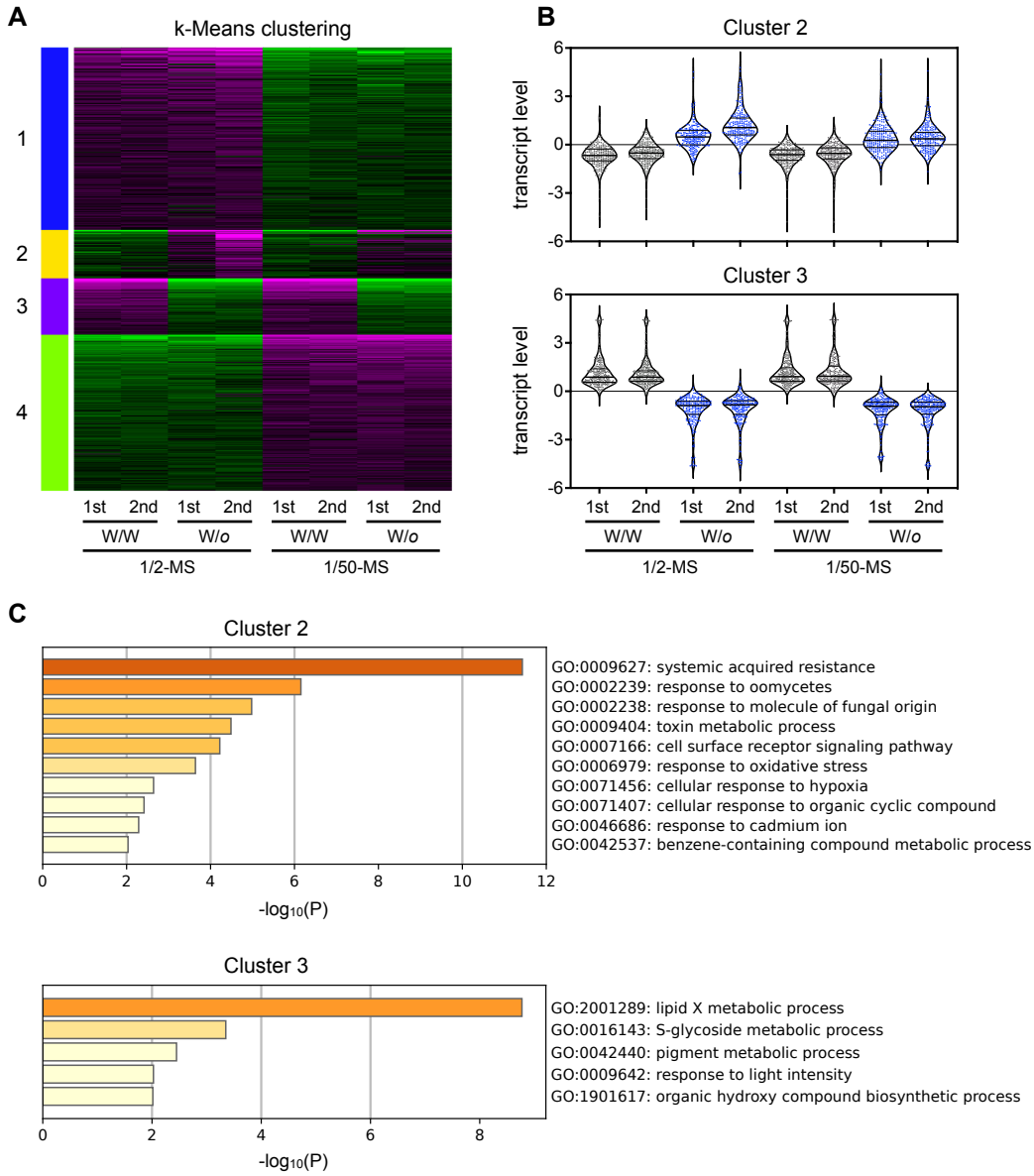
A
k-Means clustering
1
2
3
4
1st 2nd 1st 2nd 1st 2nd 1st 2nd
W/W W/o W/W W/o
1/2-MS 1/50-MS
B
Cluster 2
transcript level
6
3
0
-3
-6
Cluster 3
1st 2nd 1st 2nd 1st 2nd 1st 2nd
W/W W/o W/W W/o
1/2-MS 1/50-MS
C
Cluster 2
GO:0009627: systemic acquired resistance
GO:0002239: response to oomycetes
GO:0002238: response to molecule of fungal origin
GO:0009404: toxin metabolic process
GO:0007166: cell surface receptor signaling pathway
GO:0006979: response to oxidative stress
GO:0071456: cellular response to hypoxia
GO:0071407: cellular response to organic cyclic compound
GO:0046686: response to cadmium ion
GO:0042537: benzene-containing compound metabolic process
0 2 4 6 8 10 12
-log10(P)
Cluster 3
GO:2001289: lipid X metabolic process
GO:0016143: S-glycoside metabolic process
GO:0042440: pigment metabolic process
GO:0009642: response to light intensity
GO:1901617: organic hydroxy compound biosynthetic process
0 2 4 6 8
-log10(P)